LWT - Food Science and Technology 93 (2018) 243–248

Contents lists available at ScienceDirect

LWT - Food Science and Technology

journal homepage: www.elsevier.com/locate/lwt

Flow properties of caseinomacropeptide aqueous solutions: Effect of particle size distribution, concentration, pH and temperature

Karina G. Loria[a,b], Jimena C. Aragón[c], Sofía M. Torregiani[c], Ana M.R. Pilosof[d,e], María E. Farías[a,b,d,*]

[a] Universidad Nacional de Luján, Departamento de Tecnología, Ruta 5 y 7, Luján, 6700, Buenos Aires, Argentina
[b] CIC, Comisión de Investigaciones Científicas de la Provincia de Buenos Aires, Argentina
[c] PIR, Universidad Nacional de Luján, Departamento de Tecnología, Argentina
[d] Universidad de Buenos Aires, Departamento de Industrias, Facultad de Ciencias Exactas y Naturales, Intendente Güiraldes, s/n, Ciudad Universitaria, Buenos Aires, 1428, Argentina
[e] ITAPROQ-CONICET, Universidad de Buenos Aires, Facultad de Ciencias Exactas y Naturales, Intendente Güiraldes, s/n, Ciudad Universitaria, Buenos Aires, 1428, Argentina

ARTICLE INFO

Keywords:
Caseinomacropeptide
Flow behaviour
Particle size distribution
Rheology
Beverage

ABSTRACT

The purpose of this research was to evaluate the influence of particle size distribution, pH (5.0–9.0), concentration (1–15 g/100 g.) and temperature (5–60 °C) on the steady shear flow properties of caseinomacropeptide (CMP) aqueous solutions. These measurements were carried out by using a controlled stress rheometer. Flow curves were satisfactorily fitted by the Herschel-Bulkley model. CMP solutions exhibited Newtonian flow dependence, particularly at pH values 5.0–6.0. Non-Newtonian shear thinning behaviour was observed at pH 7.0–9.0. The concentration dependence on viscosity showed two different regimes of viscosity increase (dilute and concentrated). The overlap concentration was 8 g/100 g. The temperature dependent behaviour of CMP solutions fitted to the Arrhenius model regardless pH and concentration, and the calculated activation energy was 20 kJ/mol. The flow behaviour of CMP is explained in terms of peptide-peptide and peptide-water interactions. Based on these results, CMP molecules would form spontaneously micelles at pH > 4.5 in ultrapure water.

1. Introduction

The bioactive caseinomacropeptide (CMP) is released by rennet during cheese production. In molecular terms, CMP is the 64 amino acid long C-terminal fragment of κ-casein, and fully conserved post-translational modifications (phosphorylation and glycation) of the parental protein (Thomä-Worringer, Sørensen, & López-Fandiño, 2006; Villumsen et al., 2015). Roughly 50% of bovine CMP is glycosylated being the sialic acid the terminal residue on the majority of carbohydrate chains (Brody, 2000; Mollé & Léonil, 2005; Saito & Itoh, 1992). Naturally, the whole CMP consists of an aglyco- (aCMP) and a glyco- (gCMP) fractions being their pI 4.15 and 3.15 respectively (Kreuß, Strixner, & Kulozik, 2009). It is a random coiled peptide with high conformational flexibility (Kreuß et al., 2009; Ono, Yada, Yutani, & Nakai, 1987). There are no aromatic amino acids residues in CMP thus it can be applied in diets for phenylketonuria patients (La Clair, Ney, Leod, & Etzel, 2009; Lim, van Calcar, Nelson, Gleason, & Ney, 2007; Solverson et al., 2012).

In a previous work (Farías, Martinez, & Pilosof, 2010), the formation at room temperature of self-assembled CMP structures and opaque gels at acidic pH (< 4.5) was described. The self-assembly mechanism of CMP is driven by hydrophobic and electrostatic interactions. When pH falls below 6.5 there is an increasing protonation of acidic AA side chains which would allow the interaction of the N-terminal hydrophobic domain (AA 1–5), followed by the hydrophobic domains located in the centre of the peptide chain (Kreuß et al., 2009). Consequently, CMP self-assembly to form dimers stable to pH changes occurs via interactions of hydrophobic domains at pH values below 6.5 (Farías et al., 2010). When pH further decreases below 4.5, dimers interact by electrostatic interactions to form gels over time.

This study is motivated by the use of CMP based beverages at pH > 4.5; because of its high negative charges, the peptide self-assembly is not possible. CMP self-assembly plays a central role in the formation of visible aggregates observed in acidic WPI beverages during storage (Villumsen et al., 2015). Thus, viscosity control of concentrate CMP solutions while maintain stability for a shell life is

* Corresponding author. Universidad Nacional de Luján, Departamento de Tecnología, Ruta 5 y 7, Luján, 6700, Buenos Aires, Argentina.
E-mail address: efarias@mail.unlu.edu.ar (M.E. Farías).

https://doi.org/10.1016/j.lwt.2018.03.050
Received 4 February 2018; Received in revised form 18 March 2018; Accepted 19 March 2018
Available online 21 March 2018

necessary. Flow analysis is a tool for studying physicochemical interactions between biological macromolecules including their conformational changes under the effect of temperature (Ghaouar, Elmissaoui, Aschi, & Gharbi, 2010). So, well-developed colloidal theories for spherical particles have been applied to understand the viscosity of globular protein solutions in different conditions (Zhang & Liu, 2017). However, literature search showed that information available concerning large and highly charged peptides like CMP is limited. Ahmed and Ramaswamy (2003) studied flow changes of Davisco CMP (12.5 g/100 g, pH 7.0) upon exposure to high pressures from 100 to 400 MPa for 30 min and temperatures from 20 to 80 °C for 15 min. On the other hand, Burgardt et al. (2014) analysed the flow behaviour of aqueous systems with CMP (2–10 g/100 g), with or without carboxymethylcellulose, as well at neutral pH.

Using both of viscosity and dynamic light scattering techniques, we are interested to characterize different concentration regimes and analyse the complex phenomena involved in the CMP flow behaviour in aqueous solution in order to define general criteria applicable to the design of innovative beverages. Hence, the present study addresses questions of how changes in particle size, concentration (1–15 g/100 g), pH (5.0–9.0) and temperature (5–60 °C) are related to flow properties of CMP aqueous solutions.

2. Materials and methods

2.1. Materials

BioPURE-GMP® CMP was provided from DAVISCO Foods International, Inc. (Le Sueur, MN, USA). Its composition was determined according to AOAC (2005): protein 79.9 ± 2.7 g/100 g. (N x 7.07, Kjeldahl method), ash 6.16 ± 0.01 g/100 g and moisture 7.78 ± 0.01 g/100 g. The content of fat was insignificant (Soxhlet extraction method). The amount of carbohydrate 6.1 g/100 g was obtained from the difference between 100 and the sum of the other components. The calcium and sodium contents were determined with an AAnalyst 200 PerkinElmer atomic absorption spectrometer (Shelton, CT, USA). The mineral composition analysed was (mg kg^{-1}): 9500 Na and 6820 Ca.

Peptide solutions (1–15 g/100 g), were prepared by suspending the CMP powder in Milli-Q ultrapure water (2.3 ± 0.1 µS cm^{-1}). Solutions were stirred at room temperature for at least 4 h and left overnight at 4 °C prior to usage. The pH was adjusted at different values (5.0; 5.5; 6.0; 6.6; 7.0; 7.5; 8.0 and 9.0) using NaOH or HCl 1 equi/L to avoid dilution. Sodium azide (0.02 g/100 g) was added as a preservative.

2.2. Particle size measurement

Dynamic light scattering (DLS) measurements were carried out using a Zetasizer Nano-Zs (Malvern Instruments, Malvern, UK) as reported previously in Farías and Pilosof (2016). The assay was performed for triplicate on three individual samples at 25 °C. The samples used for DLS were filtered through a 0.45, 0.22 and 0.02 µm microfilter (Whatman International Ltd., Maidstone, England) before use.

2.3. Steady shear rheological measurements

The steady shear rheological measurements were performed using a rotational test on a rheometer (Physica MCR 301, Anton Paar, Germany). The measuring system was equipped with a cone and plate geometry CP50 (50 mm diameter, 1° cone angle and 0.099 mm gap). Samples of 560 ìL were poured into the determination platform of the instrument. Temperature was controlled by a water bath in combination with a Peltier heating system. The exposed edge of the sample was coated with silicone oil to minimize the loss of water for studies conducted at temperature higher than 25 °C. The experiments were performed in triplicate.

Steady flow tests of CMP aqueous solutions at different concentrations from 1 to 15 g/100 g were run using a linear shear rate ramp from 0 to 300 s^{-1} over temperature range from 5 to 60 °C. Flow curves assays were performed until 60 °C because a maximum effect of temperature is reached (Martinez, Farías, & Pilosof, 2011). Tests were made in automatic mode to guarantee the steady state at each shear rate to be reached.

2.4. Data analysis

Shear stress and apparent viscosity (η) were recorded as a function of shear rate. The experimental data were fitted to the Herschel-Bulkley model (Ahmed & Ramaswamy, 2003).

The temperature dependence of apparent viscosity at 100 s^{-1} (η_{100}) was fitted with the Arrhenius model (Arogundade, Eromosele, Eromosele, & Ademuyiwa, 2011; Ma, Lin, Chen, Zhao, & Zhang, 2014; Ni et al., 2016). The flow activation energy was determined from the plot of η_{100} versus T^{-1}.

Regressions were done using GraphPad Prims v7.0 (GraphPad Software, San Diego, CA, USA). Statistical analysis was performed using one-way analysis of variance (ANOVA) and Tukey's post hoc test at significance level of $p < 0.05$.

3. Results and discussion

3.1. Effect of CMP concentration on flow behaviour

The predominant population in the volume size distribution (Fig. 1 B) was, for all CMP concentrations at pH 7.0, that corresponding to the lower size peaks in Fig. 1A, revealing that most of the particles are below 5 nm. The predominant form of CMP at pH 6.5–7.0 had a hydrodynamic diameter near 2.3 nm that corresponded to the monomeric form (7.5 kDa), but the width of the first peak shows that dimers, trimers and tetramers were also present (Farías et al., 2010). As shown in Fig. 1A, the height of the predominant first peak in the intensity size distribution in becomes gradually lowered with increasing its concentration and concomitantly the volume size distributions in Fig. 1B shifted to slightly larger sizes. Thus, the DLS results pointed out that even at high CMP concentrations (8 g/100 g) the monomeric form was predominant.

Fig. 2A shows the steady flow curves of CMP solutions at different concentrations ranging from 1.0 to 15.0 g/100 g at pH 7.0 and 25 °C. In terms of determination coefficients (R^2), Herschel-Bulkley model gave a good fitting with $R^2 > 0.998$. *K* indexes increased from 0.001 to 0.010 Pa.s^n as CMP concentration increased, but this trend was more noticeable above 8 g/100 g (Fig. 2B). The analysis of the flow behaviour index (*n*) suggested that CMP solutions exhibited a Newtonian behaviour (Fig. 2C), as it had seen in solutions of low molecular materials (Kale, Yadav, Hicks, & Hanah, 2015). However at 15 g/100 g, CMP showed a slightly tendency to shear thinning behaviour, with *n* value falling close to 0.95. Also, the CMP samples exhibited very low yield stress as 0.02 Pa (1–12 g/100 g) and 0.11 Pa (15 g/100 g). Newtonian flow behaviour at low concentrations but a shear-thinning behaviour at high concentrations (> 140 g L^{-1}) has been reported for concentrated sodium caseinate suspensions (Pitkowski, Durand, & Nicolai, 2008). A reasonable good agreement was obtained when our results were compared with those reported in previous studies of Ahmed and Ramaswamy (2003) (at atmospheric pressure and 20 °C, 12.5 g/100 g CMP concentration), despite the different geometry and equipment used. Other authors (Burgardt et al., 2014) reported a shear thickening behaviour at pH 6.5 regardless the CMP concentration. Despite the similar origin of the CMP powder, the *n* indexes were between 1.15 and 1.32. They had attributed their results to the dimeric form and small aggregates present in CMP solutions at pH 6.5. This discrepancy in results could be caused by shear rate coverage, equipment, analytical assumptions and environmental conditions, namely presence of ions.

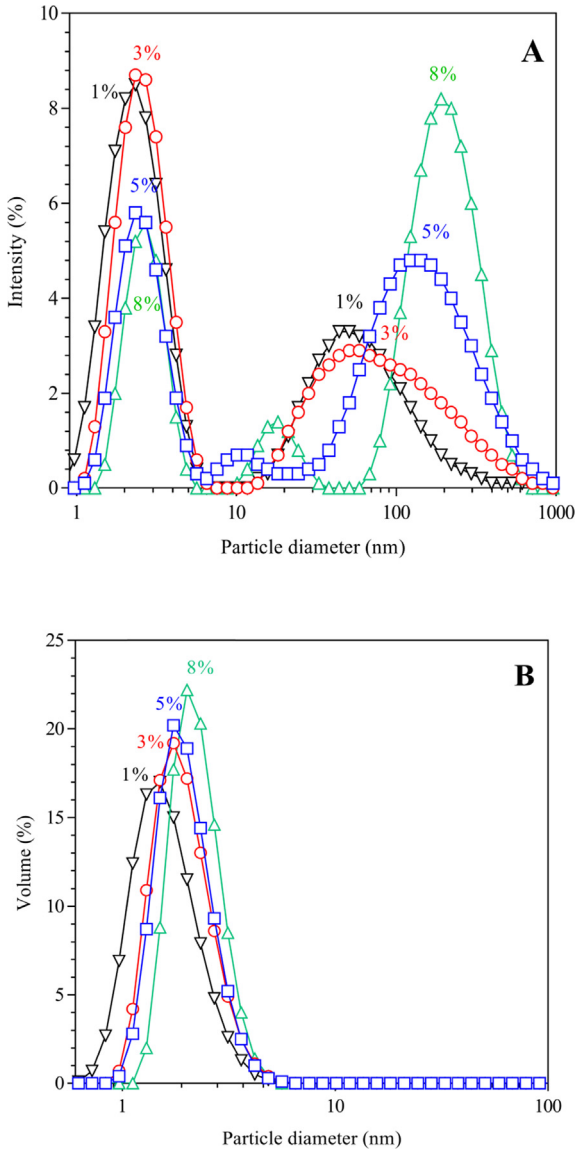

Fig. 1. Intensity (A) and Volume (B) size distribution for CMP solutions at pH 7.0 at 25 °C at different concentrations: 1 (▽); 3 (○); 5 (□) and 8 g/100 g. (△).

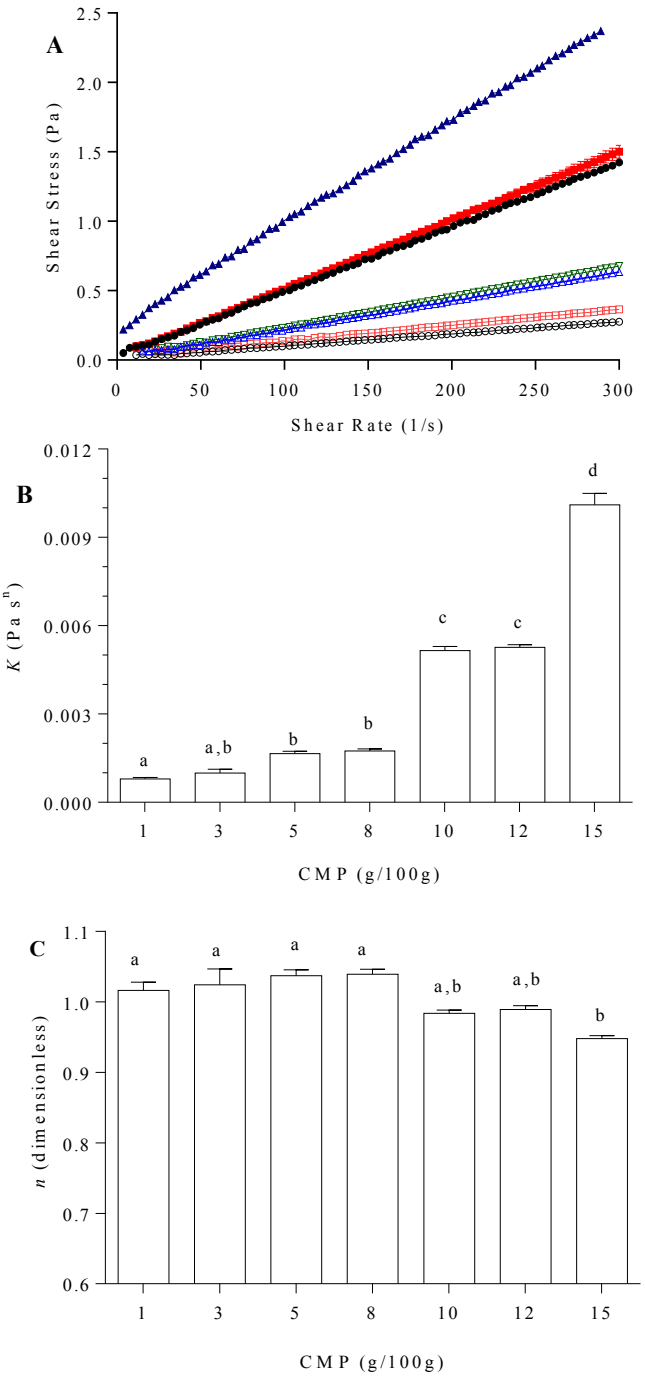

Fig. 2. A) Shear flow behaviour of CMP solutions at pH 7.0 and 25 °C. CMP concentrations: 1 (○); 3 (□); 5 (△); 8 (▽); 10 (●); 12 (■) and 15 g/100 g. (▲). Herschel-Bulkley model fitting parameters as function of CMP concentrations: B) *K* and C) *n*. Different superscript letters indicate significant difference ($p < 0.05$) ($n = 3$). Bars represent standard deviation.

As general trend, viscosity increased for increasing CMP concentration. Fig. 3 shows the double log plots for the shear viscosity at 100 s^{-1} (η_{100}) versus CMP concentration where two linear regimes (dilute and concentrated) can be observed. The intersection of these linear regimes is designated as C^*, the so-called overlap concentration (Kale et al., 2015), and it is characterized by an abrupt change in the slope of the viscosity versus concentration curve (de Kruif, Bhatt, Anema, & Coker, 2015). Thus, it can be simple to determine C^*, separating the dilute and the concentrated regime. C^* value for CMP solutions was around 8 g/100 g. Below C^*, CMP molecules would behave as individual 'particles' in solution. In dilute solutions, each molecule is randomly separated and intermolecular interactions can be ignored (Huang, Zeng, Xiong, & Huang, 2016).

To investigate the concentration dependence of CMP viscosities, it was accepted that $\eta_{100} \sim C^b$, where C is the protein concentration (g/100 g), and *b* is a characteristic coefficient that describes the rate of change of viscosity with concentration (Zhang, Arrighi, Campbell, Lonchamp, & Euston, 2016). Above C^*, the viscosity of the solution increased much more rapidly (b = 1.77) with concentration than below C^* (b = 0.45). At concentrated regime, a higher b value was found, where random peptide molecules started to overlap and interpenetrate one another. Zhang et al. (2016) conducted a similar study using whey protein concentrate (WPC). They found a C^* value of 12 g/100 g and b values of 0.38 and 1.37 for dilute and concentrated regime, respectively, which are similar values to those found here.

3.2. Effect of pH on flow behaviour

This study showed that the flow behaviour of CMP depends on pH (Fig. 4). It can be seen in Fig. 4A that τ_o values were negligible at pH 5.0 to 6.0 (≈0.02 Pa), however, they were 10 times higher for the other pH

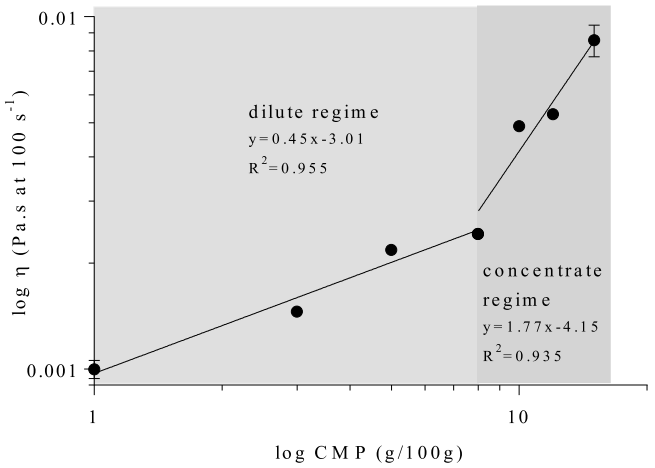

Fig. 3. Concentration dependence of apparent viscosity at 100 s^{-1} (η_{100}) expressed as a log-log plot. The lines indicate the best fit lines of diluted and concentrated regimes. Bars represent standard deviation.

values (≈0.15 Pa). Increasing pH of CMP solutions from 6.6 to 9.0 increased *K* values (Fig. 4B). Nevertheless, there are no significant differences between pH 5.0 and 6.0 ($p > 0.05$). Concerning *n* index (Fig. 4C), this parameter reveals Newtonian flow behaviour when pH goes from 5.5 to 6.6, and a clear shear-thinning behaviour within pH 7.0 and 9.0. Morales, Martinez and Pilosof (2017) reported that the viscosity of sodium caseinate solutions at pH 7 was significantly higher than that of CMP, but at pH 5.5 they exhibited comparable viscosities.

A possible explanation of these differences of flow behaviour is related to the increasing of water binding capacity. Thus, the increase of pH value converted carboxyl groups into ionized forms, thereby improving the water binding properties (Li et al., 2017). The highly solvated molecules present may be progressively sheared away with increasing shear rate causing a reduction in the apparent viscosity (Arogundade et al., 2011). The viscosity increase is in fact connected with the protein–water interactions, leading to a higher solvent immobilization than protein–protein interaction (Barreto et al., 2003). Concordantly, samples at pH within pH 7.0 and 9.0 were very similar sized (Z-ave ≈ 13.1 nm) and the individual CMP molecules (monomers of 2.3 nm) showed a tendency to keep each other at distance (Fig. 5 A and B).

In order to investigate the influence of the size distribution on the flow behaviour within pH 5.0 to 6.0, Fig. 5 C and D are showed. Different intensity and volume size distributions are apparent at pH 5.0 (Z-ave 6.2 nm, predominant form: tetramers of 4.2 nm) than pH 6.0 (Z-ave 9.8 nm, predominant form: monomers). However, the lower size peak of CMP at pH 6.0, broadening from 1.3 to 5.6 nm, confirmed the presence of more dimers and tetramers than pH 8.0 and 9.0 (1.1–4.8 nm). It is reported in the literature that the tetrameric form of CMP is more hydrophobic than the dimeric and monomeric forms (Mikkelsen et al., 2005). Hence, viscosity of solutions at pH 5.0–6.0 did no depend on the pH or the association form of CMP. The tendency to Newtonian flow behaviour at pH within 5.0–6.0 would be explained by the increased hydrophobicity which decreases the binding of water molecules to the peptide.

3.3. Effect of temperature on viscosity

Regarding the effect of temperature on steady shear flow curves at a fixed concentration of 15 g/100 g (Fig. 6), it resulted in a significant decrease in shear viscosities (η) for all pH tested, indicating that CMP aqueous solutions flowed more easily due to the increase of temperature. The decrease of η can be attributed to the interactions of the molecules in solution, which are weaker at higher temperature (Karataş & Arslan, 2016; Ma et al., 2014). This effect can be attributed to the

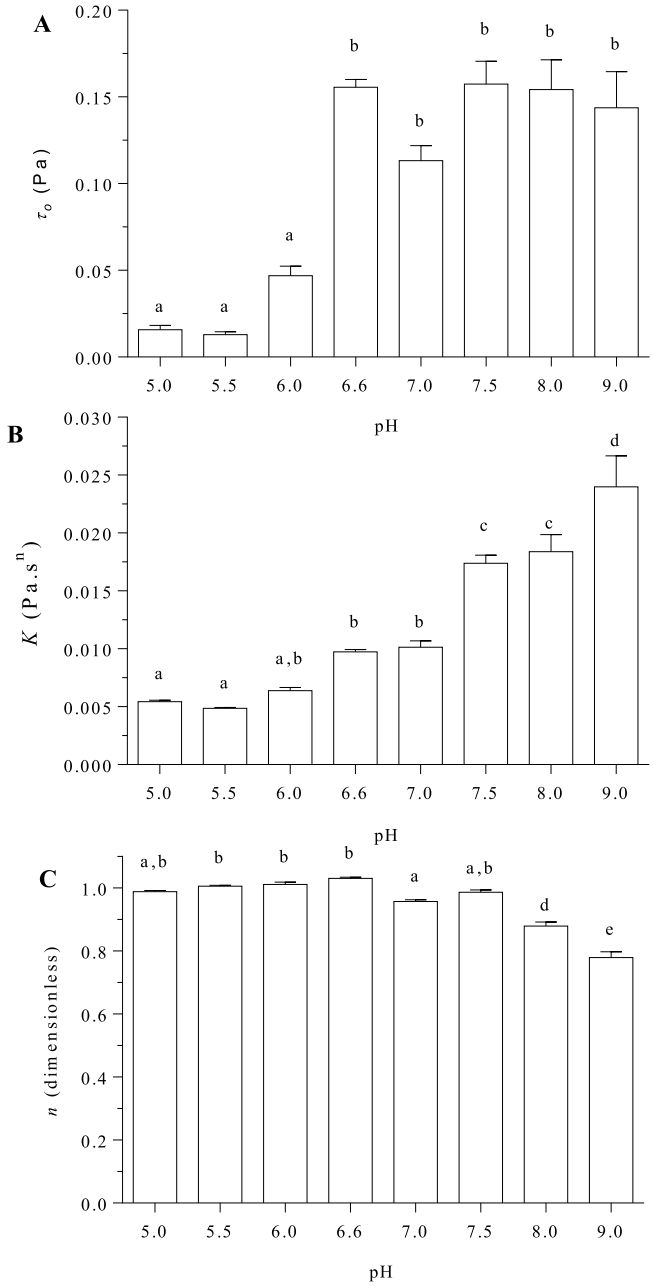

Fig. 4. Herschel-Bulkley model fitting parameters: τ_o (A), *K* (B) and *n* (C) at different pH values for 15 g/100 g CMP concentration at 25 °C. Different superscript letters indicate significant differences ($p < 0.05$). Bars represent standard deviation.

increase in the kinetic energy of molecules which could diminish interaction among them (Arogundade et al., 2011). Hydrogen bonding, electrostatic and van der Waals are exothermic in nature and are destabilizes at high temperature, while hydrophobic interactions are endothermic and are stabilize at high temperature though not indefinitely (Arogundade et al., 2011). It is important to say that the solutions at pH > 4.5 did not show any change in the particle size distributions upon heating as it was reported by Martinez et al. (2011). This behaviour distinguishes the CMP from the other whey proteins where the high temperature favours the denaturation that increases the viscosity (Gómez-Arellano et al., 2017). There is no significant change in *n* values at pH range studied even with increasing temperature (data not shown). However, *n* values depended on concentration at a given temperature and pH (Fig. 4).

The effect of temperature on apparent viscosity of CMP solutions at

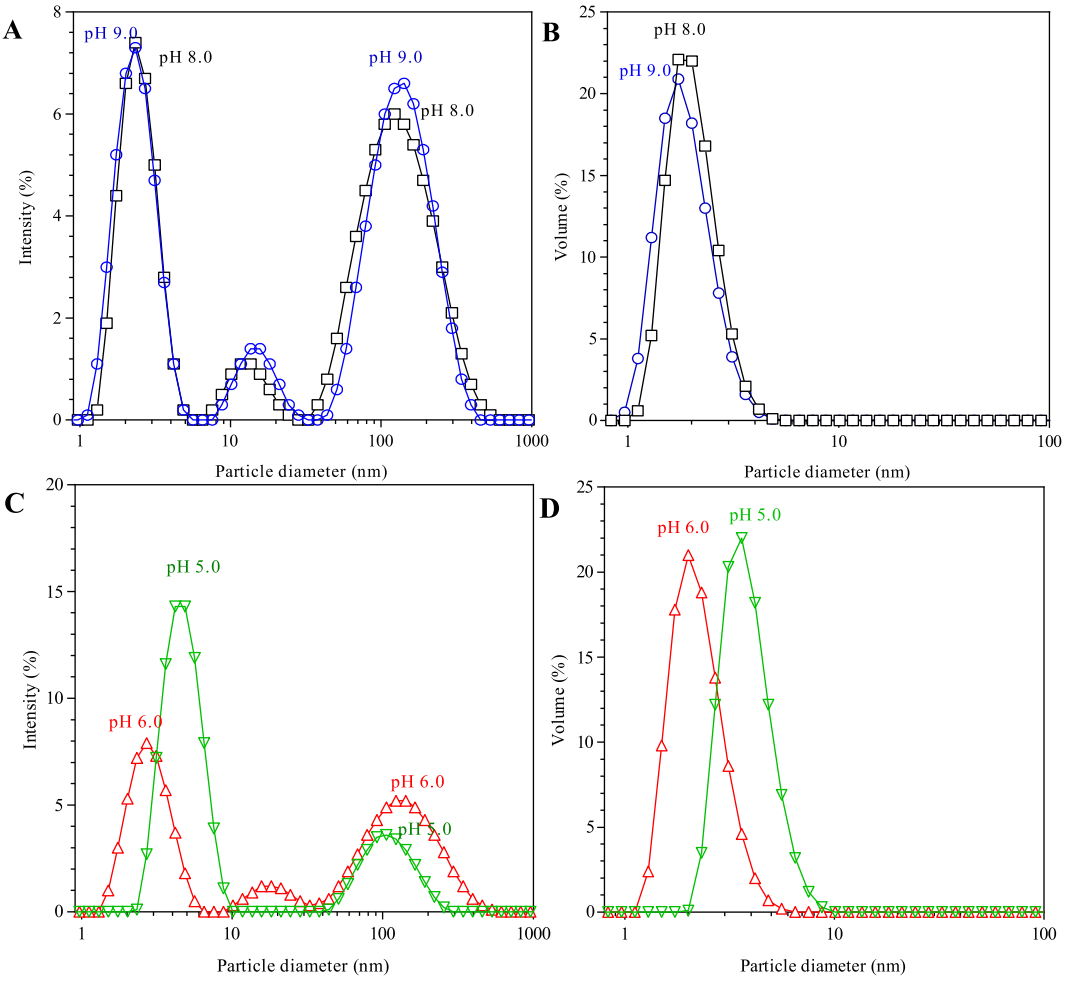

Fig. 5. Intensity (A and C) and volume (B and D) size distributions for 5 g/100 g. CMP solutions at 25 °C at pH: 8.0 (□) and 9.0 (○) (A and B); 5.0 (▽) and 6.0 (△) (C and D).

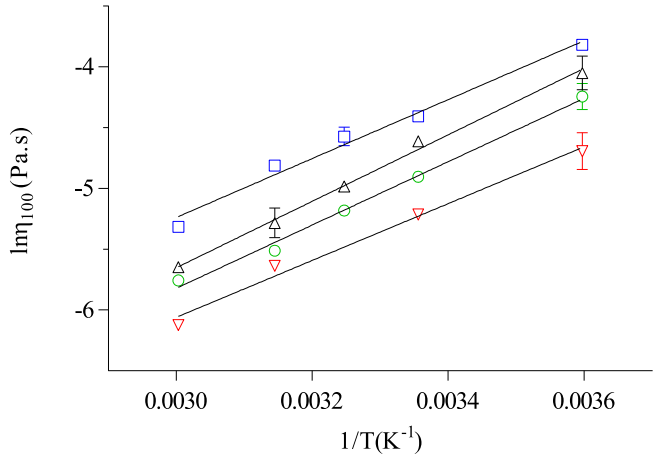

Fig. 6. Dependence of apparent viscosity at 100 s^{-1} (η_{100}) on temperature for 15 g/100 g. CMP solutions at different pH values: 5.0 (▽); 6.0 (○); 8.0 (□) and 9.0 (△). Bars represent standard deviation.

Table 1
Flow activation energy (*Ea*) and R^2 for 15 g/100 g CMP solutions obtained at viscosity of 100 s^{-1}.

	pH 5.0	pH 6.0	pH 8.0	pH 9.0
Ea (kJ/mol)	19.4 ± 1.5[a]	21.6 ± 1.0[a]	20.1 ± 1.5[a]	22.7 ± 0.9[a]
R^2	0.988	0.994	0.984	0.996

Data are means ± standard deviations (n = 3). Different superscript letters indicate significant differences ($p < 0.05$).

Table 2
Flow activation energy (*Ea*) and R^2 for CMP solutions at pH 7obtained at viscosity of 100 s^{-1}.

	5 g/100 g	15 g/100 g
Ea (kJ/mol)	20.4 ± 0.9[a]	18.6 ± 2.3[a]
R^2	0.998	0.955

Data are means ± standard deviations (n = 3). Different superscript letters indicate significant differences ($p < 0.05$).

a specified shear rate, η_{100}, can be described by the Arrhenius relationship, in which the apparent viscosity decreases exponentially with temperature (Fig. 6). The higher viscosity value for this shear rate corresponded to pH 8.0, followed by pH 9.0, 6.0 and 5.0. The flow activation energy, *Ea*, reflects the measure of viscosity sensitivity to temperature changes (Karataş & Arslan, 2016). The corresponding values of *Ea* and R^2 are shown in Table 1. *Ea* was independent of pH values being approximately 20 kJ/mol. The magnitude of *Ea* was higher than that reported for 12.5 g/100 g CMP solutions at pH 7.0 (12.4 kJ/mol) (Ahmed & Ramaswamy, 2003). This difference could be due to the temperature range used in that work (20–80 °C). On the other hand, *Ea* values were also independent of concentration (5 and 15 g/100 g) as shown Table 2. Peptide concentration would be expected to exert an effect; however, the results indicated that CMP aqueous solutions were

sensitive to temperature changes regardless concentration. CMP solutions had big viscosity changes with increasing temperature in comparison with sodium caseinate. Barreto et al. (2003) reported an *Ea* of sodium caseinate (13 g/100 g) of 12.1 kJ/mol which increases with solution concentration.

Micelles are self-assembling structures of amphiphilic molecules as biopolymers or surfactants. Ponton, Schott, and Quemada (1998) studied the rheological behaviour of flexible elongated micelles. Considering the shear thinning behaviour of micelles, its flow energy of activation (≈16 kJ/mol), its independence of mass fraction and its temperature independent power law exponent (Ponton et al., 1998) and based on our results, we can hypothesizer that CMP molecules spontaneously form micelles at pH > 4.5. The shear thinning behaviour at pH 7.0–9.0 could be explained in terms of the orientation of the micelles in the flow direction as well the peptide-water interactions. This interpretation is in line with previously showed presence of negligible peaks of 15 and 100 nm in CMP intensity distributions (Figs. 1 and 5). According to Martinez, Carrera Sánchez, Patino & Pilosof (2009), the surface pressure isotherms of CMP solutions showed a sigmoidal behaviour which is typical for biopolymers and surfactants. Also, its adsorption kinetics at the air–water interface was not driven by the diffusion step, characteristic of low-molecular-weight surfactants.

4. Conclusions

CMP solutions exhibited Newtonian flow dependence, particularly at pH values 5.0–6.0, where the hydrophobic interactions were predominant. Non-Newtonian shear thinning behaviour was observed at pH 7.0–9.0, explained by the electrostatic repulsion and the peptide-water interaction. From the concentration dependence, the overlap concentration was found to be 8 g/100 g, indicating the transition from a dilute solution to a concentrated regime. The temperature dependent behaviour of CMP solutions fitted to the Arrhenius model regardless pH and concentration. Based on these results, CMP molecules would form spontaneously micelles at pH > 4.5 in ultrapure water. The results of this study point out the importance of reducing pH (between 5 and 6) and heating to control the viscosity of highly concentrate CMP beverages. Further work is underway to understand the effect of cations on CMP flow properties.

Acknowledgments

This research was supported by Universidad Nacional de Luján, Agencia Nacional de Promoción Científica y Tecnológica de la República Argentina (Project: PICT-2014-1402) and Comisión de Investigaciones Científicas of the Province of Buenos Aires (CIC). K.G.L. received an posgrade fellowship from CIC. The authors would like to acknowledge Silvina Ríos for technical support in the composition analysis; Gustavo Gómez and Andrés Pighín for performing the mineral composition determinations.

References

Ahmed, J., & Ramaswamy, H. S. (2003). Effect of high-hydrostatic pressure and temperature on rheological characteristics of glycomacropeptide. *Journal of Dairy Science, 86*, 1535–1540.

AOAC (2005). *Official methods of analysis of association of official analytical chemists international* (18th ed.). USA: AOAC.

Arogundade, L. A., Eromosele, C. O., Eromosele, I. C., & Ademuyiwa, O. (2011). Rheological properties of African yam bean (*Sphenostylis stenocarpa* Hochst. Ex A. Rich.) calcium proteinate and isoelectric protein isolates. *Lebensmittel-Wissenschaft und -Technologie- Food Science and Technology, 44*, 524–534.

Barreto, P. L. M., Roeder, J., Crespo, J. S., Maciel, G. R., Terenzi, H., Pires, A. T. N., et al. (2003). Effect of concentration, temperature and plasticizer content on rheological properties of sodium caseinate and sodium caseinate/sorbitol solutions and glass transition of their films. *Food Chemistry, 82*, 425–431.

Brody, E. P. (2000). Biological activities of bovine glycomacropeptide. *British Journal of Nutrition, 84*, 39–46.

Burgardt, V. C. F., Oliveira, D. F., Evseev, I. G., Coelho, A. R., Haminiuk, C. W. I., & Waszczynskyj, N. (2014). Influence of concentration and pH in caseinomacropeptide and carboxymethylcellulose interaction. *Food Hydrocolloids, 35*, 170–180.

Farías, M. E., Martinez, M. J., & Pilosof, A. M. R. (2010). Casein glycomacropeptide pH-dependent self-assembly and cold gelation. *International Dairy Journal, 20*, 79–88.

Farías, M. E., & Pilosof, A. M. R. (2016). The influence of acid type on self-assembly, rheological and textural properties of caseinomacropeptide. *International Dairy Journal, 55*, 17–25.

Ghaouar, N., Elmissaoui, S., Aschi, A., & Gharbi, A. (2010). Concentration regimes and denaturation effects on the conformational changes of α-chymotrypsin by viscosity and dynamic light scattering measurements. *International Journal of Biological Macromolecules, 47*, 425–430.

Gómez-Arellano, A., Jiménez-Islas, H., Castrejón-González, E. O., Medina-Torres, L., Dendooven, L., & Escamilla-Silva, E. M. (2017). Rheological behaviour of sesame (Sesamum indicum L.) protein dispersions. *Food and Bioproducts Processing, 106*, 201–208.

Huang, J., Zeng, S., Xiong, S., & Huang, Q. (2016). Steady, dynamic, and creep-recovery rheological properties of myofibrillar protein from grass carp muscle. *Food Hydrocolloids, 61*, 48–56.

Kale, M. S., Yadav, M. P., Hicks, K. B., & Hanah, K. (2015). Concentration and shear rate dependence of solution viscosity for arabinoxylans from different sources. *Food Hydrocolloids, 47*, 178–183.

Karataş, M., & Arslan, N. (2016). Flow behaviours of cellulose and carboxymethyl cellulose from grapefruit peel. *Food Hydrocolloids, 58*, 235–245.

Kreuß, M., Strixner, T., & Kulozik, U. (2009). The effect of glycosylation on the interfacial properties of bovine caseinomacropeptide. *Food Hydrocolloids, 23*, 1818–1826.

de Kruif, C. G., Bhatt, H., Anema, S. G., & Coker, C. (2015). Rheology of caseinate fractions in relation to their water holding capacity. *Food Hydrocolloids, 51*, 503–511.

La Clair, C., Ney, D., Leod, E. M., & Etzel, M. (2009). Purification and use of glycomacropeptide for nutritional management of phenylketonuria. *Journal of Food Science, 74*, 199–206.

Li, S., Donner, E., Thompson, M., Zhang, Y., Rempel, C., & Liu, Q. (2017). Preparation of branched canola protein isolate and effects of molecular architecture on solution flow properties. *Lebensmittel-Wissenschaft und -Technologie- Food Science and Technology, 79*, 287–293.

Lim, K., van Calcar, S. C., Nelson, K. L., Gleason, S. T., & Ney, D. M. (2007). Acceptable low-phenylalanine foods and beverages can be made with glycomacropeptide from cheese whey for individuals with PKU. *Molecular Genetics and Metabolism, 92*, 176–178.

Ma, J., Lin, Y., Chen, X., Zhao, B., & Zhang, J. (2014). Flow behavior, thixotropy and dynamical viscoelasticity of sodium alginate aqueous solutions. *Food Hydrocolloids, 38*, 119–128.

Martinez, M. J., Carrera Sánchez, C., Patino, J. M. R., & Pilosof, A. M. R. (2009). Bulk and interfacial behaviour of caseinoglycomacropeptide (GMP). *Colloids and Surfaces B: Biointerfaces, 71*, 230–237.

Martinez, M. J., Farías, M. E., & Pilosof, A. M. R. (2011). Casein glycomacropeptide pH-driven self-assembly and gelation upon heating. *Food Hydrocolloids, 25*, 860–867.

Mikkelsen, T. L., Frøkiær, H., Topp, C., Bonomi, F., Iametti, S., Picariello, G., et al. (2005). Caseinomacropeptide self-association is dependent on whether the peptide is free or restricted in κ-casein. *Journal of Dairy Science, 88*, 4228–4238.

Mollé, D., & Léonil, J. (2005). Quantitative determination of bovine κ-casein macropeptide in dairy products by Liquid chromatography/Electrospray coupled to mass spectrometry (LC-ESI/MS) and Liquid chromatography/Electrospray coupled to tamdem mass spectrometry (LC-ESI/MS/MS). *International Dairy Journal, 15*, 419–428.

Morales, R., Martinez, M. J., & Pilosof, A. M. R. (2017). Synergistic effect of casein glycomacropeptide on sodium caseinate foaming properties. *Colloids and Surfaces B: Biointerfaces, 159*, 501–508.

Ni, X., Chen, W., Xiao, M., Wu, K., Kuang, Y., Corke, H., et al. (2016). Physical stability and rheological properties of konjac glucomannan-ethyl cellulose mixed emulsions. *International Journal of Biological Macromolecules, 92*, 423–430.

Ono, T., Yada, R., Yutani, K., & Nakai, S. (1987). Comparison of conformations of κ-casein, para-κ-casein and glycomacropeptide. *Biochimica et Biophysica Acta (BBA) - Protein Structure and Molecular Enzymology, 911*, 318–325.

Pitkowski, A., Durand, D., & Nicolai, T. (2008). Structure and dynamical mechanical properties of suspensions of sodium caseinate. *Journal of Colloid and Interface Science, 326*, 96–102.

Ponton, A., Schott, C., & Quemada, D. (1998). Rheological behavior of flexible elongated micelles: Temperature effect in an isotropic phase. *Colloids and Surfaces A: Physicochemical and Engineering Aspects, 145*, 37–45.

Saito, T., & Itoh, T. (1992). Variations and distributions of O-glycosidically linked sugar chains in bovine κ-casein A. *Journal of Dairy Science, 75*, 1768–1774.

Solverson, P., Murali, S. G., Brinkman, A. S., Nelson, D. W., Clayton, M. K., Yen, C. L., et al. (2012). Glycomacropeptide, a low-phenylalanine protein isolated from cheese whey, supports growth and attenuates metabolic stress in the murine model of phenylketonuria. *American Journal of Physiology. Endocrinology and Metabolism, 302*, 31.

Thomä-Worringer, C., Sørensen, J., & López-Fandiño, R. (2006). Health effects and technological features of caseinomacropeptide. *International Dairy Journal, 16*, 1324–1333.

Villumsen, N. S., Jensen, H. B., Thu Le, T. T., Møller, H. S., Nordvang, R. T., Nielsen, L. R., et al. (2015). Self-assembly of caseinomacropeptide as a potential key mechanism in the formation of visible storage induced aggregates in acidic whey protein isolate dispersions. *International Dairy Journal, 49*, 8–15.

Zhang, Z., Arrighi, V., Campbell, L., Lonchamp, J., & Euston, S. R. (2016). Properties of partially denatured whey protein products 2: Solution flow properties. *Food Hydrocolloids, 56*, 218–226.

Zhang, Z., & Liu, Y. (2017). Recent progresses of understanding the viscosity of concentrated protein solutions. *Current Opinion in Chemical Engineering, 16*, 48–55.